PNAS
www.pnas.org

Supplementary Information: Materials and Methods, Figures, and Tables for

Disruption of a key ligand-H-bond network drives dissociative properties in Vamorolone for Duchenne Muscular Dystrophy Treatment.

Xu Liu[a], Yashuo Wang[a], Jennifer S. Gutierrez[a], Jesse M. Damsker[b], Kanneboyina Nagaraju[b,c], Eric P. Hoffman[b,c] and Eric A. Ortlund[a,1]

[a]Emory University, Atlanta, GR, 30303

[b]ReveraGen Biopharma, LLC, Rockville, MD, 20850

[c]Binghamton University- SUNY, Binghamton, NY, USA, 13902

[1]Correspondence should be addressed to Eric A. Ortlund, E-mail: eortlun@emory.edu

This PDF file includes:

Supplementary text (SI Materials and Methods)

Figures S1 to S8

Table S1

SI Materials and Methods

Protein expression and purification. hGR N564A and AncGR2 N33A mutations were produced using QuikChange site-directed mutagenesis kit (Agilent) and constructs were verified by Sanger sequencing prior to use. All AncGR2 LBD constructs were expressed in *E. coli* BL21 cells, induced by 0.3 mM isopropyl-1-thio-D-galactopyranoside (IPTG) and 50 μM drug [hydrocortisone (HCY); prednisolone (PRED); C_{21}-desacetyl deflazacort (dDFZ); or vamorolone (VAM)] at 16 °C, and further grown overnight. AncGR2 LBD with or without a maltose-binding protein (MBP)-fused His tag were purified as previously reported (1). AncGR2 LBD with a N-terminal His-SUMO tag was purified by His-Trap affinity chromatography (GE Healthcare). Protein was further purified by Superdex 75 size exclusion chromatography in a buffer containing 20 mM HEPES pH 7.4, 150 mM NaCl, 1 mM EDTA, 5 mM DTT, and 0.005 % Tween-20 for Microarray Assay for Real-time Coregulator-Nuclear receptor Interaction (MARCoNI).

Crystallization, data collection and structure determination. GR2 LBD was concentrated to 4 mg/ml with two-fold excess PGC1α NR Box 2 peptide (NH_2-EEPSLLKKLLLAPA-COO^-) or SHP peptide (NH_2-QGAASRPAILYALLSSSLK-COO^-) in a buffer containing 20 mM HEPES (pH 7.4), 200 mM NaCl, and 5 % glycerol. Crystals were grown by the hanging-drop vapor diffusion method at 16 °C. Crystals of the AncGR2 LBD-PRED were formed in 0.2 M ammonium acetate, 3.0 M sodium formate, and 0.1 M HEPES 8.0. AncGR2 LBD-dDFZ crystals were obtained in 0.2 M ammonium acetate, 2.5 M sodium formate, and 0.1 M Tris pH 8.5. AncGR2 LBD-VAM was crystalized in 25% PEG 300 and 0.1 M Tris pH 8.5. Crystals were flash-frozen in liquid nitrogen after soaking for 5 s in mother liquor containing 25% glycerol.

X-ray diffraction data were collected on the South East Regional Collaborative Access Team (SER-CAT) beamline 22-ID at the Advanced Photon Source (APS) at Argonne National Laboratories at 100 K and processed using HKL-2000 (2). The structures were determined by molecular replacement using the structure of AncGR2 LBD-Dex (PDB: 3GN8) as an initial search model (3) with program Phaser-MR (4). Repeated rounds of manual refitting and crystallographic refinement were performed using PHENIX (v1.12) and COOT (5). PyMOL (v1.8.2) was used to perform alignments and generate figures (Schrödinger, LLC). Hydrogen bonds and hydrophobic contacts were identified by Ligplot (v.4.5.3) (6).

Ligand binding and coregulator binding assays. 100 nM MBP-fused GR2LBD preincubated with 12 nM FAM-labelled DEX was used for competition ligand binding assays with increasing amounts of unlabeled PRED, dDFZ or HCY added into the solution. The fluorescence polarization (FP) signal (Ex=485 nm; Em=528 nm) was recorded using a BioTek Neo plate-reader (Winooski, VT). Three technical replicates and three biological replicates were conducted, and graphical compilations of all data were created. Binding data were fit with one-site Ki-fit curve in GraphPad Prism v8 (GraphPad, Inc).

Different N-terminal FAM-labelled peptides at 50 nM was used for coregulator binding assays with increasing amount of GR2 LBD titrated into the solution. The FP signal was recorded as mentioned above. Three technical replicates and three biological replicates were conducted and graphs were compilations of all data collected. Binding data were fit with a one-site binding curve in GraphPad Prism v8 (1).

MARCoNI. The assay mixture for hGR consists of 1 nM GST-tagged hGR LBD (aa 521-777, Invitrogen), 25 nM ALEXA-488 conjugated GST antibody (Fisher Scientific), and 5 mM DTT, in Coregulator buffer F (Invitrogen) in the presence of solvent only (2% DMSO) or 1 μM drug as indicated. The reaction mixture for GR2 consists of 10 nM His-SUMO-tagged GR2 WT or N33A (expressed in the presence of drug as indicated), 25 nM ALEXA-488 conjugated penta-His antibody (Qiagen), 5 mM DTT, in reaction buffer (as mentioned above) in the presence of additional 1 μM of the respective drug to preserve full loading. Experiments were conducted on a PamStation96 (PamGene) at room temperature. In short, PamChip arrays (PamGene) were blocked for 20 cycles with 1% BSA (Calbiochem) in Tris-buffered saline (TBS), incubated for 40 minutes with 25 μl assay mix using 3 arrays per mix and finally rinsed twice with TBS. Binding on array (tif) images were quantified with BioNavigator software (PamGene). A modulation index, i.e. the log-transformed ratio of binding in presence over absence (solvent) of compound, was calculated for each interaction. Significance of the modulation was assessed using Student's t-Test and FDR post hoc correction.

Differential scanning fluorimetry (DSF). GR2 LBD in 20 mM Tris (pH 7.4), 300 mM NaCl, and 5 % glycerol at 10 μM was used for DSF assays. Protein was incubated with 50 μM PRED, dDFZ, or VAM in the presence of 50 μM coregulator peptides and SYPRO® orange dye (Sigma) at a final dilution of

1:1000. The peptide sequences used were as follows: Tif2 NR Box 3 (NH2-KENALLRYLLDKDD-COO^-), SMRT (NH2-TNMGLEAIIRKALMGKY-COO^-) and NCoR ID2 (NH2-DPASNLGLEDIIRKALMGSFDDK-COO^-). Temperature scans were performed from 25 °C to 95 °C at a rate of 0.5 °C/min using a StepOne Plus Real Time PCR System (ThermoFisher) with fluorescence monitored using the ROX filter (602 nm). Three technical replicates and three biological replicates were conducted. The data were normalized and fit to a two-state model with a single transition between native and denatured protein using Boltzmann sigmoidal curve as previously described (1, 7).

Hydrogen-deuterium exchange-mass spectrometry (HDX-MS). HDX-MS was performed on AncGR2 LBD-PRED and -VAM at 2 mg/ml using a UPLC coupled with a Q-Tof Premier MS and a robotic autosampler (Waters Corp, Milford, MA) as previously described (1). Briefly, triplicate exchange reactions were initialized by diluting each protein sample 1:7 (v/v) into 10 mM phosphate buffer in 99.9 % D_2O for 0, 10, 100, 1000 and 10000 seconds. Precooled quenching buffer [100 mM phosphate, 0.5 M tris(2-carboxyethyl) phosphine, 0.8% formic acid, and 2% acetonitrile, pH 2.5] was added to stop the exchange reaction prior to exposure to an online pepsin column (Waters Corp, Milford, MA). Peptides were separated by a C18 UPLC column and analyzed by MS. Peptides were identified using ProteinLynx Global SERVER™ (PLGS) and the deuterium incorporation data were processed in DynamX (v3.0). The HDX difference between different states was calculated by comparing the relative fractional uptake for each residue at a given time.

Molecular dynamics simulations. All 1000 ns molecular dynamics simulations were performed with Amber18 (8) using a 2 fs timestep as previously described (1). Briefly, AncGR2 LBD-PRED, -dDFZ, and -VAM complexes were solvated in an octahedral box of TIP3P water with 10 Å buffer surrounding it, supplemented with Na^+ and Cl^- ions to a final concentration of 150 mM to neutralize the protein. All bonds between heavy atoms and hydrogens were fixed with the SHAKE algorithm (9). Root mean square fluctuations (RMSF) were calculated on Cα atoms of protein residues for each frame in the trajectory using the initial structure as the reference. Carma program and NetworkView plugin in VMD (10) were utilized for producing the dynamic network by calculating the cartesian covariance and correlation between two nodes (11). The edge distances were derived from pairwise correlations as a measure of

communication within the network. Suboptimal paths were identified using the Floyd-Warshall algorithm (12) and analyzed by subopt program in the VMD NetworkView plugin (10).

Reporter gene assays. Reporter gene assays were performed as previously reported (13). Briefly, HeLa cells were maintained and passaged in α-minimal essential medium (Life Technologies) supplemented with 10 % stripped FBS (Invitrogen). Cells were grown in 96-well plates to 70 % confluence and transfected with 10 ng of hGR WT or N564A mutant, 50 ng of SGK and IL8 κBRE firefly luciferase reporter, and 1 ng of Renilla luciferase reporter under the control of the constitutively active pRL-CMV promoter using with FuGeneHD (Roche Applied Science). Cells were treated with different concentrations of drugs or DMSO 24 hours after transfection in triplicate. Renilla and firefly luciferase activities were measured 24 hours after drug treatment using the DualGlo kit (Promega) by a BioTek Neo plate-reader (Winooski, VT).

GR dimerization assays. NanoLuc luciferase-based bioluminescence resonance energy transfer ($BRET^n$) assay and Protein-Fragment Complementation Assay (NanoPCA) were carried out as previously described(14-16). For NanoPCA, GR WT and GR A458T/I628A monomeric mutant (Mon) were subcloned into NanoLuc luciferase (NLuc)-PCA vectors containing the N- or C-NLuc fragments using Gateway cloning system (Invitrogen, CA). For $BRET^n$ assay, GR WT and Mon were cloned into BRET vectors containing a NLuc or Venus-tag. All plasmids generated were confirmed by sequencing. HEK293T cells were maintained as HeLa cells used in reporter gene assays. For NanoPCA, cells were transfected with 1 ng of both N- and C-NLuc-fused GR (WT or Mon) or GR with empty NLuc vectors and then treated with drugs at 1 μM or DMSO in triplicate 24 hours later. Luciferase activities were measured 24 hours after drug treatment using the NanoGlo kit (Promega) by a BioTek Neo plate-reader (Winooski, VT). The PCA signal (signal/background ratios) were calculated as a ratio of averaged experiment signal to the higher averaged background obtained from both empty vector controls. For BRET assay, cells were transfected with 5 ng of Nluc-GR and 320 ng of venus-GR or pcDNA (as the no venus control). After drug treatment, the donor luminescence signal at 450 nm and acceptor emission signal at 530 nm were measured using the NanoGlo kit (Promega) by a BioTek Neo plate-reader (Winooski, VT). The $BRET^n$ signal is the ratio of intensity of acceptor signal over donor signal and the net $BRET^n$ is the difference in $BRET^n$ signal of Nluc-GR/venus-GR pair and the NLuc-GR/pcDNA control.

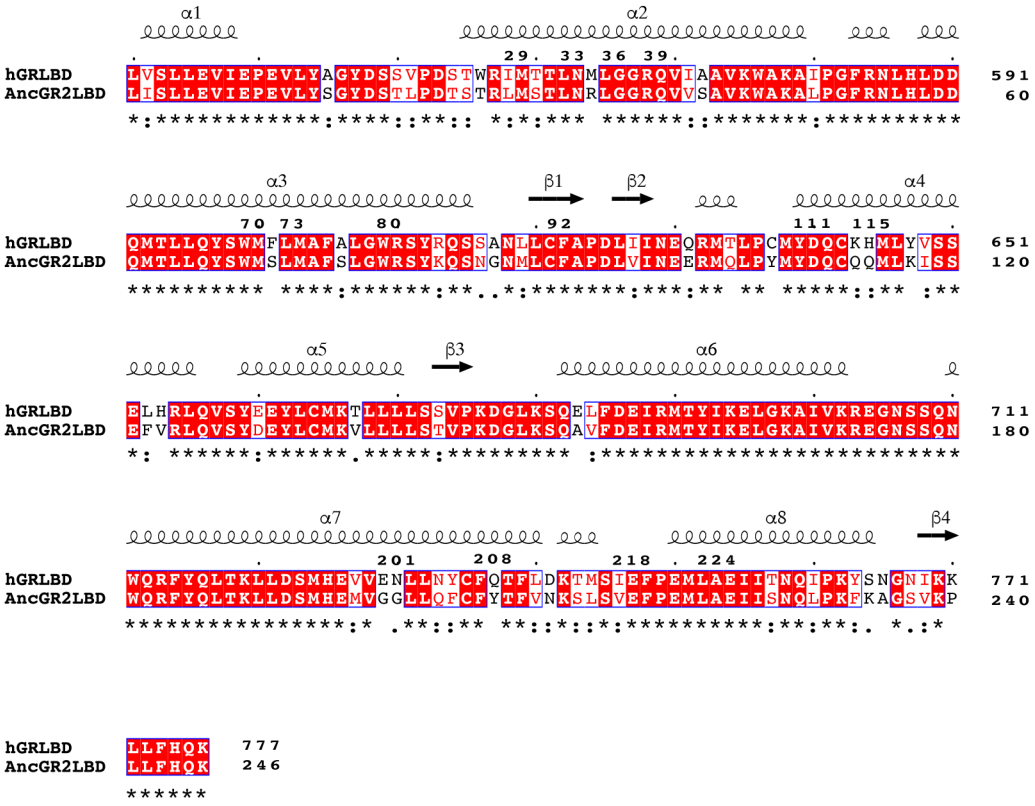

Figure S1. Sequence alignment of hGR and AncGR2 LBD. Identical residues are highlighted with a red background while similar residues are displayed in red text. Secondary structure elements are indicated at the top. Number of residues participating H-bonding and hydrophobic interactions with ligands (related to Figure 2) and the allosteric communication from ligand to AF-H (related to Figure 5) are labeled. This figure was generated by *ClustalW* and *ESPript.*

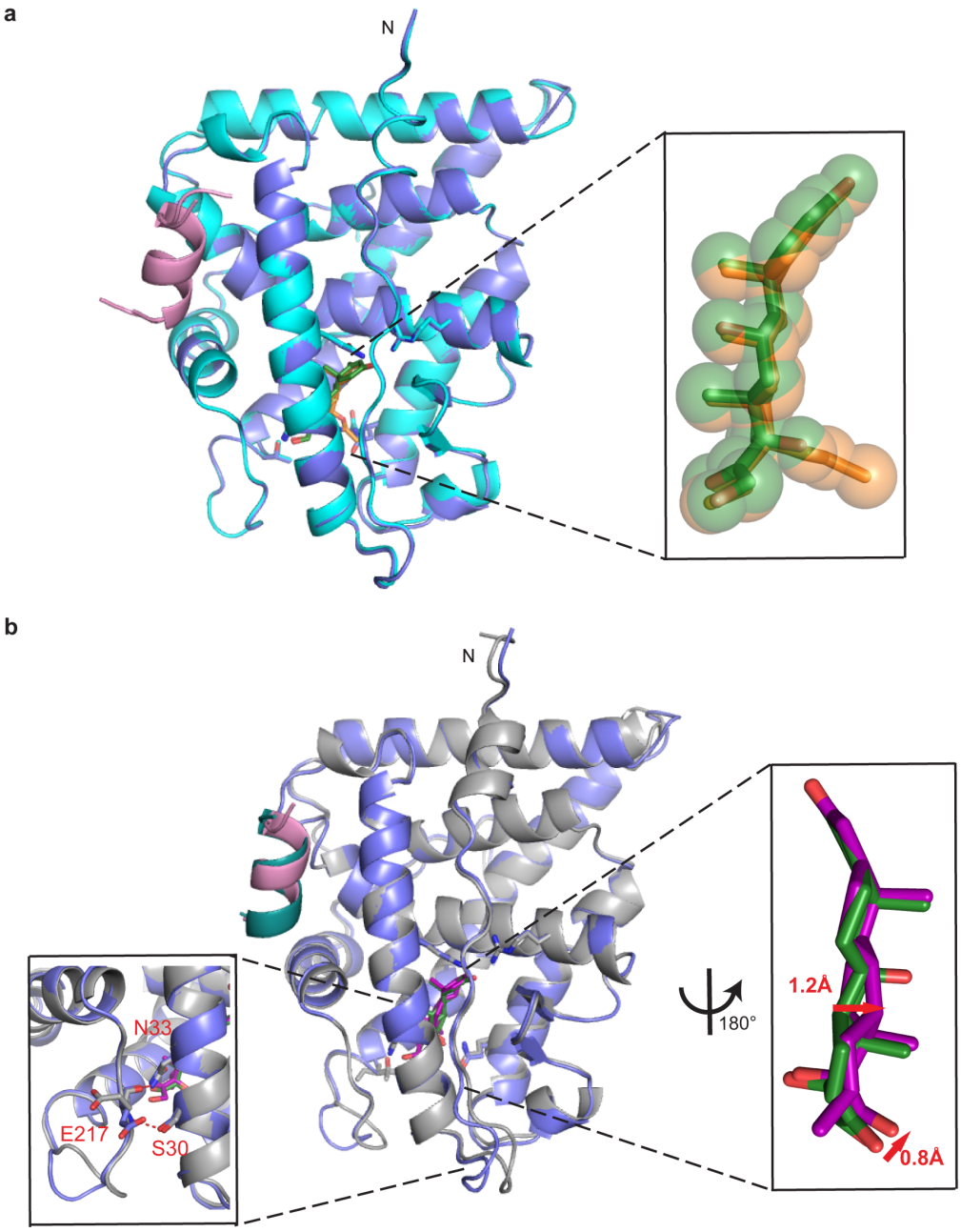

Figure S2. Structural comparison between AncGR2 LBD in complexes with prednisolone, C21-desacetyl deflazacort and vamorolone. (**a**). Structural overlay of the prednisolone (PRED, marine)- and C_{21}-desacetyl deflazacort (dDFZ, cyan)- bound AncGR2 LBD. Inset: overlay of compound PRED and dDFZ. (**b**). Structural overlay of the PRED (marine)- and vamorolone (VAM, grey)- bound AncGR2 LBD. Inset (left): hydrogen bonding between H3 and the loop preceding AF-2; Inset (right): overlay of compound PRED and VAM.

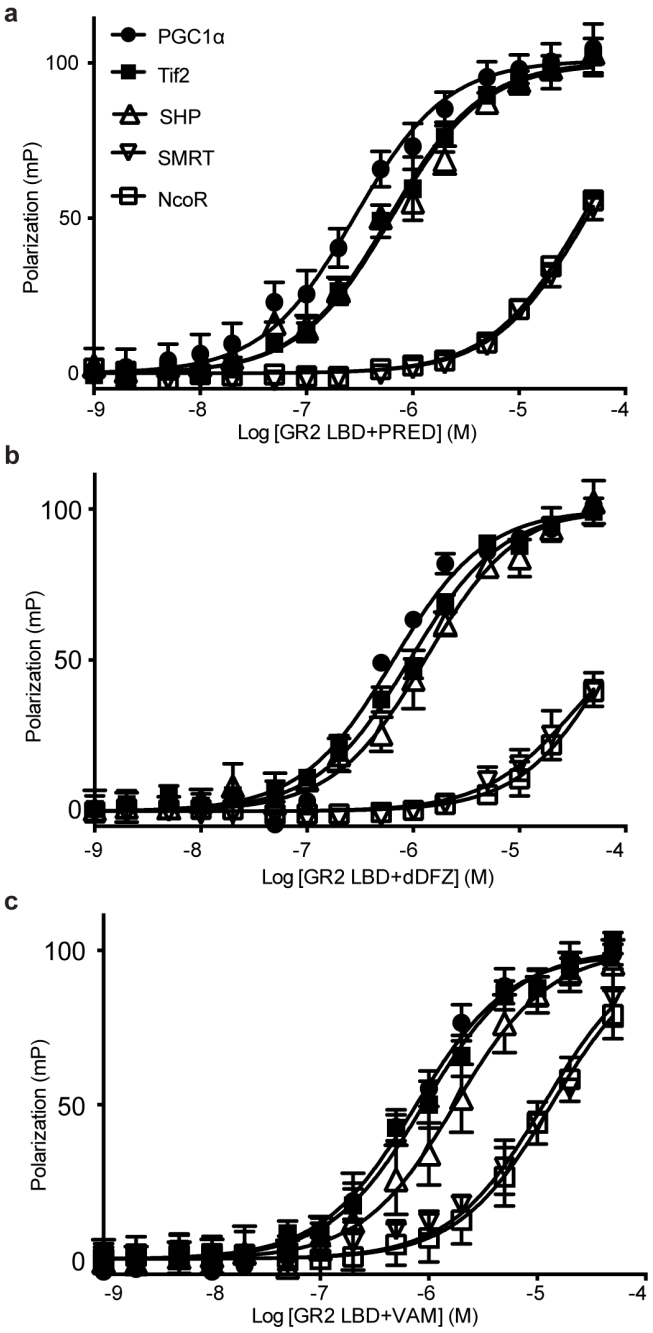

Figure S3. Coregulator binding profiles for AncGR2 LBD in complex with ligands. AncGR2 LBD with PRED (**a**), dDFZ (**b**), and VAM (**c**) was titrated into various FAM-labelled coregulator peptides to monitor fluorescence polarization signal changes to determine binding affinities. These data are represented as mean ± (S.D.) from three replicates and from three independent experiments.

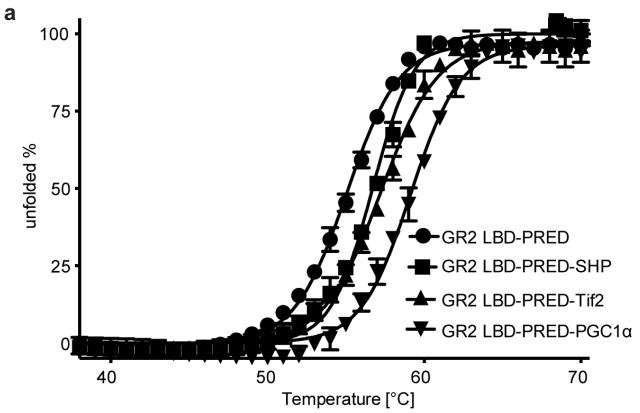

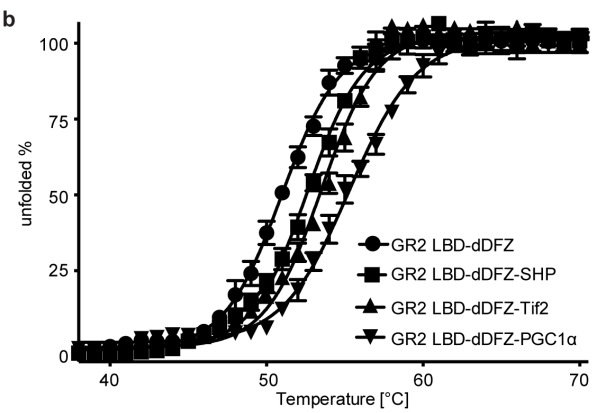

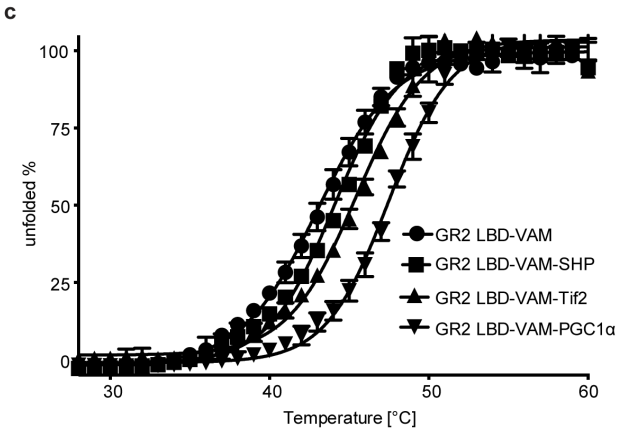

d

	Ligand		
coregulator	PRED	dDFZ	VAM
Apo	54.0 [52.6,55.7]	51.7 [49.2,53.1]	43.7 [41.4,45.9]
SHP	55.7 [54.1,57.3]	53.2 [51.4,55.8]	45.0 [42.7,47.6]
Tif2	56.2 [54.8,58.5]	54.1 [52.5,56.4]	45.8 [42.3,47.7]
PGC1α	58.1 [56.3,60.8]	55.4 [52.8,57.5]	47.2 [44.8,49.6]
NCoR	54.1 [52.4,56.2]	51.6 [49.5,53.8]	43.9 [41.4,45.7]
SMRT	53.8 [52.2,56.5]	51.5 [49.3,53.4]	43.5 [40.9,45.6]

Figure S4. Thermostability of AncGR2 LBD bound to PRED, dDFZ and VAM and in complex with different coregulators. (**a**-**c**) Thermal unfolding curves of AncGR2 LBD bound to PRED (**a**), dDFZ (**b**), and VAM (**c**) in presence of coactivators. These data are represented as mean ± (S.D.) from three replicates and from three independent experiments. (**d**). Thermostability for various coregulators bound to AncGR2 LBD with different ligands are expressed as Tm (°C) with 95% confidence interval from three replicates and from three independent experiments.

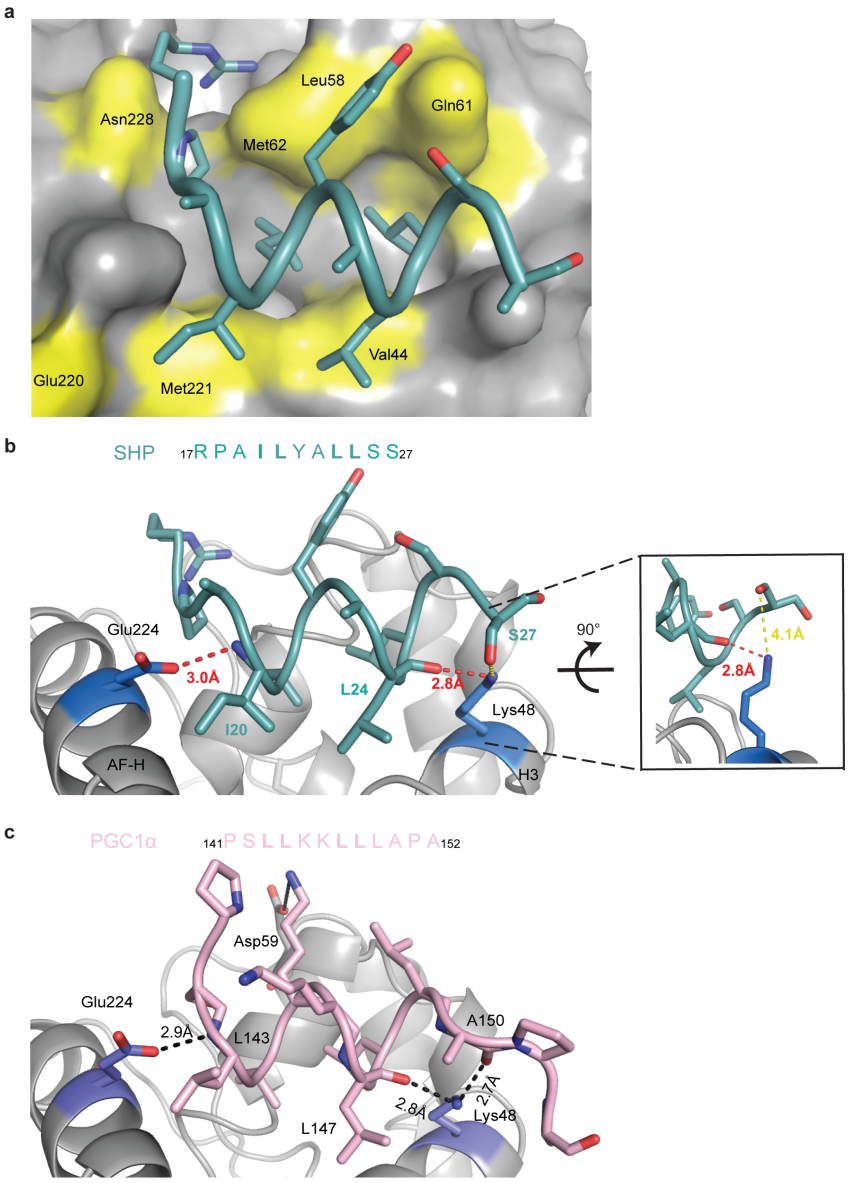

Figure S5. Recognition of SHP at the AncGR2 LBD AF-2 surface. (**a**) SHP binds to AncGR2 LBD AF-2 and forms extensive hydrophobic contacts with LBD (participating residues colored in yellow). (**b**) Primary charge clamps are mediated by Glu224 and Lys48 (shown in blue) to hold SHP in place. (**c**) Stronger charge clamp is formed between Lys 48 and A150, analogous to S27 in SHP, in the PGC1α binding as indicated by shorter hydrogen bond length.

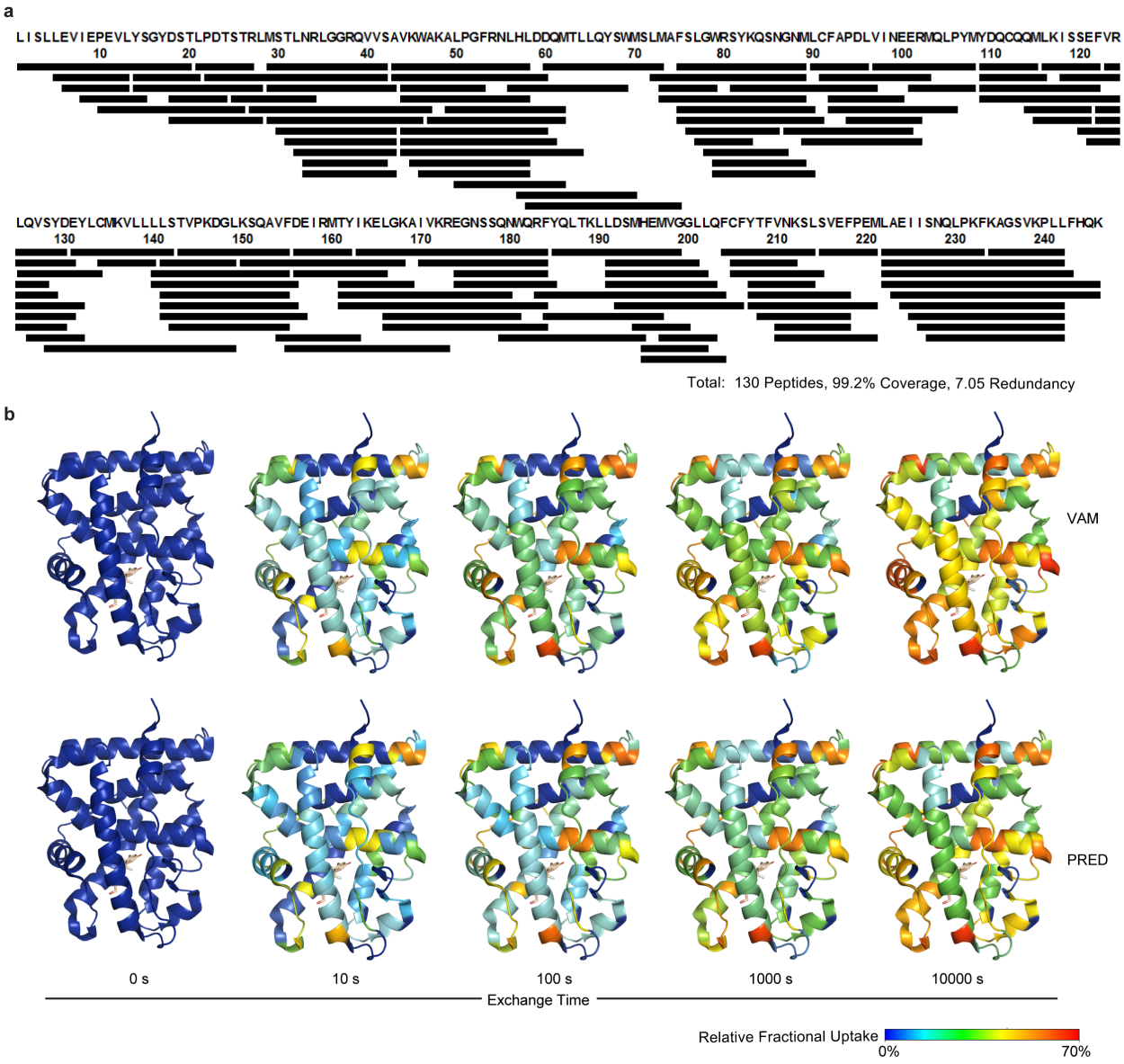

Figure S6. HDX-MS analysis of AncGR2LBD in complex with PRED and VAM. (**a**) Sequence map of peptic fragments identified in HDX-MS show 99 % coverage of AncGR2 LBD. (**b**) Relative fractional deuterium uptake mapped onto the structure of AncGR2 LBD with VAM or PRED. The relative deuterium uptake is colored along the continuous gradient from blue to red, with their intensity scaling to the magnitude.

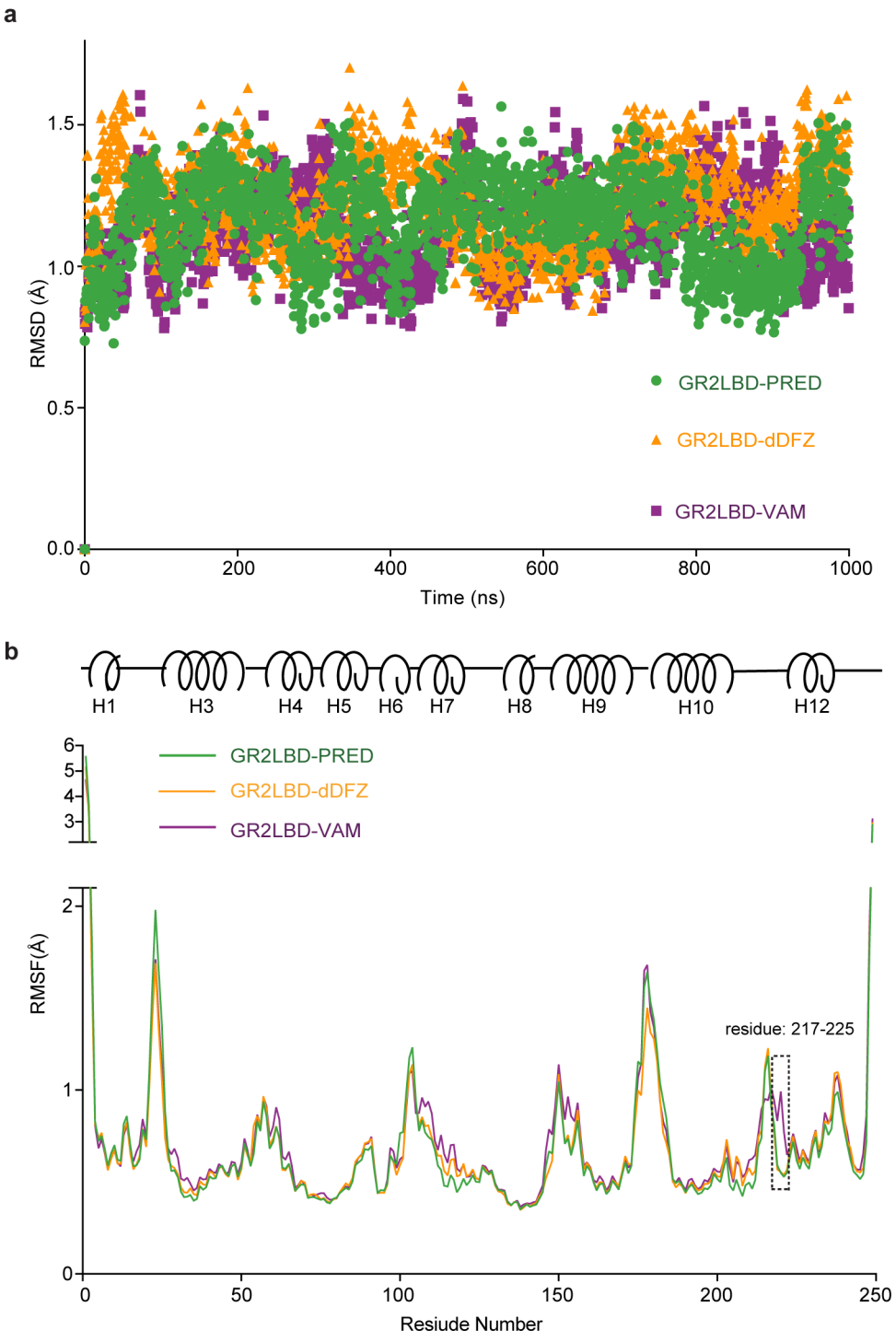

Figure S7. Cα RMSDs (a) and RMSFs (b) during simulations of AncGR2 LBD in complexes with PRED, dDFZ, and VAM, respectively. Residue 217-225 are highlighted in RMSF plot.

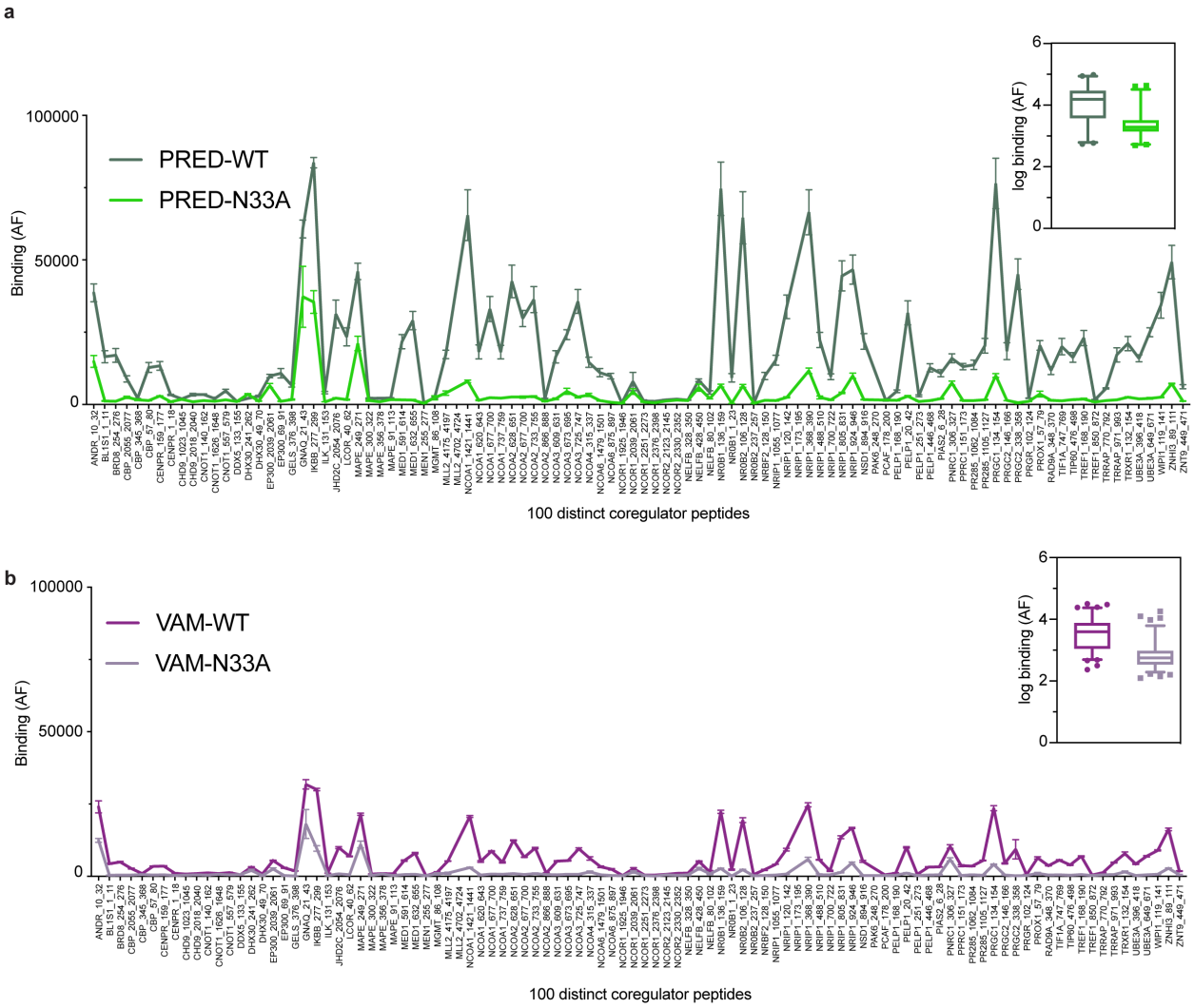

Figure S8. Effects of N33A mutation in AncGR2 LBD on coregulator binding monitored by MARCoNI. (**a**-**b**) Superposition of coregulator binding data of WT with that of N33A mutant of AncGR2 LBD in complexes with PRED (**a**) and VAM (**b**). Insets are box-and-whisker plot of Log binding of coregulators between AncGR2 WT and N33A. The line in the box is plotted at the median of all the coregulator binding whereas the whiskers are the 2.5 and 97.5 percentiles.

Table S1. X-ray Data Collection and Refinement Statistics

	AncGR2 LBD - PRED-PGC1α	AncGR2 LBD - dDFZ-PGC1α	AncGR2 LBD - VAM-SHP
Data Collection			
Space Group	C 2 2 2_1	C 2 2 2_1	C 1 2 1
Unit Cell Dimension			
a, b, c (Å)	a=71.1, b=96.1, c=108.0	a=71.7, b=96.5, c=107.5.	a=87.1, b=52.9, c=69.7.
α, β, γ (°)	90, 90, 90	90, 90, 90	90, 90, 90
Resolution (Å)	1.60 (1.66-1.60) *	1.45 (1.50-1.45)	1.59 (1.64 -1.59)
R_{pim}	0.058 (0.386)	0.069 (0.560)	0.081 (0.444)
CC ½	0.952 (0.765)	0.971 (0.571)	0.921 (0.684)
I/σ	13.3 (2.3)	10.7 (1.8)	10.9 (1.3)
Completeness	98.7 (93.9)	99.7 (99.1)	96.6 (87.4)
Redundancy	12.0 (9.6)	12.0 (8.2)	5.5 (3.2)
Refinement			
No. Reflections	48001 (4531)	66028 (6507)	37223 (3352)
Rwork/Rfree	17.4/18.7	17.5/19.7	18.4/21.3
No. Atoms			
Protein	2214	2248	2203
Ligand	44	47	50
Water	148	175	61
B-factors			
Protein	39.0	32.3	34.3
ligand	41.5	42.3	37.3
Water	49.8	46.5	37.0
R.M.S. deviations			
Bond lengths (Å)	0.01	0.01	0.01
Bond angles (°)	0.86	1.24	0.95
Ramachandran plot (%)			
Most favored	96.6	97.7	98.1
Outliers	0	0	0

*Values in the parentheses are for the highest resolution shell.

(PRED= prednisolone; dDFZ= C_{21}-desacetyl deflazacort; VAM= vamorolone)

References

1. Liu X, Wang Y, & Ortlund EA (2019) First High-Resolution Crystal Structures of the Glucocorticoid Receptor Ligand-Binding Domain-Peroxisome Proliferator-Activated gamma Coactivator 1-alpha Complex with Endogenous and Synthetic Glucocorticoids. *Mol Pharmacol* 96(4):408-417.
2. Otwinowski Z & Minor W (1997) Processing of X-ray diffraction data collected in oscillation mode. *Methods Enzymol* 276:307-326.
3. Bridgham JT, Ortlund EA, & Thornton JW (2009) An epistatic ratchet constrains the direction of glucocorticoid receptor evolution. *Nature* 461(7263):515-519.
4. Adams PD*, et al.* (2010) PHENIX: a comprehensive Python-based system for macromolecular structure solution. *Acta Crystallogr D Biol Crystallogr* 66(Pt 2):213-221.
5. Emsley P & Cowtan K (2004) Coot: model-building tools for molecular graphics. *Acta Crystallogr D Biol Crystallogr* 60(Pt 12 Pt 1):2126-2132.
6. Wallace AC, Laskowski RA, & Thornton JM (1995) LIGPLOT: a program to generate schematic diagrams of protein-ligand interactions. *Protein Eng* 8(2):127-134.
7. Weikum ER, Okafor CD, D'Agostino EH, Colucci JK, & Ortlund EA (2017) Structural Analysis of the Glucocorticoid Receptor Ligand-Binding Domain in Complex with Triamcinolone Acetonide and a Fragment of the Atypical Coregulator, Small Heterodimer Partner. *Mol Pharmacol* 92(1):12-21.
8. D.A. Case IYB-S, S.R. Brozell, D.S. Cerutti, T.E. Cheatham, III, V.W.D. Cruzeiro, T.A. Darden, R.E. Duke, D. Ghoreishi, M.K. Gilson, H. Gohlke, A.W. Goetz, D. Greene, R Harris, N. Homeyer, S. Izadi, A. Kovalenko, T. Kurtzman, T.S. Lee, S. LeGrand, P. Li, C. Lin, J. Liu, T. Luchko, R. Luo, D.J. Mermelstein, K.M. Merz, Y. Miao, G. Monard, C. Nguyen, H. Nguyen, I. Omelyan, A. Onufriev, F. Pan, R. Qi, D.R. Roe, A. Roitberg, C. Sagui, S. Schott-Verdugo, J. Shen, C.L. Simmerling, J. Smith, R. Salomon-Ferrer, J. Swails, R.C. Walker, J. Wang, H. Wei, R.M. Wolf, X. Wu, L. Xiao, D.M. York and P.A. Kollman (2018) AMBER 2018. *University of California, San Francisco*.
9. Ryckaert J-P, Ciccotti G, & Berendsen HJ (1977) Numerical integration of the cartesian equations of motion of a system with constraints: molecular dynamics of n-alkanes. *Journal of Computational Physics* 23(3):327-341.
10. Humphrey W, Dalke A, & Schulten K (1996) VMD: visual molecular dynamics. *J Mol Graph* 14(1):33-38, 27-38.
11. Glykos NM (2006) Software news and updates. Carma: a molecular dynamics analysis program. *J Comput Chem* 27(14):1765-1768.
12. Floyd RW (1962) Algorithm-97 - Shortest Path. *Commun Acm* 5(6):345-345.
13. Hudson WH*, et al.* (2018) Cryptic glucocorticoid receptor-binding sites pervade genomic NF-kappaB response elements. *Nat Commun* 9(1):1337.
14. Mo X*, et al.* (2017) AKT1, LKB1, and YAP1 Revealed as MYC Interactors with NanoLuc-Based Protein-Fragment Complementation Assay. *Mol Pharmacol* 91(4):339-347.
15. Mo XL*, et al.* (2016) Enabling systematic interrogation of protein-protein interactions in live cells with a versatile ultra-high-throughput biosensor platform. *J Mol Cell Biol* 8(3):271-281.
16. Brown NE, Blumer JB, & Hepler JR (2015) Bioluminescence resonance energy transfer to detect protein-protein interactions in live cells. *Methods Mol Biol* 1278:457-465.